5868 *Inorg. Chem.* **2010**, *49*, 5868–5875
DOI: 10.1021/ic100006a

Inorganic Chemistry
Article

Synthesis, Structures, and Magnetism of Three 1D Mn^{III} Chains with Oxazoline-Based Ligands

Yan Zhang,[†] Xiu-Teng Wang,[‡] Xiao-Man Zhang,[†] Tian-Fu Liu,*[,†] Wen-Guo Xu,[†] and Song Gao*[,‡]

[†]*Department of Chemistry, The Institute of Chemical Physics, and State Key Laboratory of Explosion Science and Technology, Beijing Institute of Technology, Beijing 100081, China, and* [‡]*Beijing National Laboratory for Molecular Sciences, State Key Laboratory of Rare Earth Materials Chemistry and Applications, College of Chemistry and Molecular Engineering, Peking University, Beijing 100871, P. R. China*

Received January 2, 2010

Three novel Mn^{III} polymers, $[Mn(phox)_2(N_3)]_n$ (**1**), $[Mn(Etphox)_2(N_3)]_n$ (**2**), and $[Mn(Etphox)_2(C_2N_3)]_n$ (**3**), using achiral ligand Hphox (Hphox = 2-(4,5-dihydrooxazol-2-yl)phenol) and chiral ligand HEtphox (HEtphox = 2-(4-ethyl-4,5-dihydrooxazol-2-yl)phenol) were synthesized and structurally and magnetically characterized. All complexes are of 1D chain structures and form 2D frameworks by weak interactions. The adjacent 1D chains of complex **1** are connected by face-to-face $\pi-\pi$ interactions, $C-H\cdots\pi$ interactions, and hydrogen bonding, which leads to the formation of a supramolecular 2D sheet structure. The three compounds show antiferromagnetic coupling between Mn^{III} ions. And compound **2** is a spin-canted weak ferromagnet with $T_N = 5.6$ K, showing metamagnetic behavior with a two-step magnetic phase transition.

Introduction

Magnetic materials based on molecular components continue to be attractive and difficult goals for organic and inorganic chemists despite more than 20 years of research on this subject.[1] The design of molecular magnetism aims to control spins in molecules and molecular assemblies.[2] The goal is to synthesize new magnetic molecular systems with expected properties owing to the flexibility of molecular chemistry and the subtleties of supramolecular interactions between the precursors.[3] Molecule-based materials provide a number of examples for understanding some fundamental phenomena better in magnetism (e.g., spin-canting, metamagnetic transition, single molecule magnet, single chain magnet, etc.).[4−9] Spin-canting means the noncollinear spin arrangements on two sublattices of an antiferromagnet. The metamagnet is the one with net moments aligned antiparallelly by weak AF interactions, which are of secondary importance.[9] A large external field could overwhelm the weak AF interactions and turn the system to a ferro-, ferri-, or weak-ferromagnetic (WF) state, depending on the

*Correspondence e-mail: liutf@bit.edu.cn (T.-F.L.), gaosong@pku.edu.cn (S.G.).

(1) Blundell, S. J.; Pratt, F. L *Condens. Matter* **2004**, *16*, R771.
(2) (a) Kahn, O. *Molecular Magnetism*; VCH: New York, 1993. (b) Miller, J. S.; Drillon, M. *Magnetism: Molecules to Materials*; Wiley−VCH: Weinheim, Germany, 2001−2005.
(3) Cyrille, T.; Ruxandra, G; Vojislav, K.; Lise-M., C.; Nikolais, O.; Geertl, J. A. R.; Michel, G.; Michel, V. *Nat. Mater.* **2008**, *7*, 729.
(4) (a) Carlin, R. L.; Van-Duyneveldt, A. J. *Magnetic Properties of Transition Metal Compounds*; Springer-Verlag: New York, 1977. (b) Carlin, R. L. *Magnetochemistry*; Springer-Verlag: Berlin, 1986.
(5) (a) Rettig, S. J.; Storr, A.; Summers, D. A.; Thompson, R. C.; Trotter, J. *J. Am. Chem. Soc.* **1997**, *119*, 8675. (b) Kurmoo, M.; Kepert, C. J. *New J. Chem.* **1998**, 1515. (c) Batten, S. R.; Jenson, P.; Kepert, C. J.; Kurmoo, M.; Moubaraki, B.; Marray, K. S.; Price, D. J. *J. Chem. Soc., Dalton Trans.* **1999**, 2987. (d) Kmety, C. R.; Huang, Q.; Lynn, J. W.; Erwin, R. W.; Manson, J. L.; McCall, S.; Crow, J. E.; Stevenson, K. L.; Miller, J. S.; Epstein, A. J. *Phys. Rev. B* **2000**, *62*, 5576. (e) Mito, M.; Kawae, T.; Takeda, K.; Takagi, S.; Matsushita, Y.; Deguchi, H.; Rawson, J. M.; Palacio, F. *Polyhedron* **2001**, *20*, 1509. (f) Richard-Plouet, M.; Vilminot, S.; Guillot, M.; Kurmoo, M. *Chem. Mater.* **2002**, *14*, 3829. (g) Wang, X. Y.; Gan, L.; Zhang, S. W.; Gao, S. *Inorg. Chem.* **2004**, *43*, 4615. (h) Wang, X.-Y.; Wei, H.-Y.; Wang, Z.-M.; Chen, Z.-D.; Gao, S. *Inorg. Chem.* **2005**, *44*, 572. (i) Salah, M. B.; Vilminot, S.; Andre, G.; Bouree-Vigneron, F.; Richard-Plouet, M.; Mhiri, T.; Kurmoo, M. *Chem. Mater.* **2005**, *17*, 2612.
(6) (a) Zora, J. A.; Seddon, K. R.; Hitchcock, P. B.; Lowe, C. B.; Shum, D. P.; Carlin, R. L. *Inorg. Chem.* **1990**, *29*, 3302. (b) Lowe, C. B.; Carlin, R. L.; Schultz, A. J.; Loong, C. K. *Inorg. Chem.* **1990**, *29*, 3308. (c) Schlueter, J. A.; Manson, J. L.; Hyzer, K. A.; Geiser, U. *Inorg. Chem.* **2004**, *43*, 4100.
(7) (a) Kurmoo, M.; Kumagai, H.; Green, M. A.; Lovett, B. W.; Blundell, S. J.; Ardavan, A.; Singleton, J. *J. Solid State Chem.* **2001**, *159*, 343. (b) Gao, E. Q.; Wang, Z. M.; Yan, C. H. *Chem. Commun.* **2003**, *14*, 1748. (c) Zeng, M. H.; Zhang, W. X.; Sun, X. Z.; Chen, X. M. *Angew. Chem., Int. Ed.* **2005**, *44*(20), 3079.
(8) (a) Herweijer, A.; de Jonge, W. J. M.; Botterman, A. C.; Bongaarts, A. L. M.; Cowen, J. A. *Phys. Rev. B* **1972**, *5*, 4618. (b) Kopinga, K.; van Vlimmeren, Q. A. G.; Bongaarts, A. L. M.; de Jonge, W. J. M. *Physica B+C* **1977**, *86−88*, 671–672. (c) Basten, J. A.; van Vlimmeren, Q. A. G.; de Jonge, W. J. M. *Phys. Rev. B* **1978**, *18*, 2179. (d) Engelfriet, D. W.; Groeneveld, W. L.; Groenendijk, H. A.; Smit, J. J.; Nap, G. M. *Z. Naturforsch.* **1980**, *35A*, 115. (e) Carlin, R. L.; Joung, K. O.; van der Bilt, A.; del Adel, H.; O'Connor, C. J.; Sinn, E. *J. Chem. Phys.* **1981**, *75*, 431. (f) Tian, Y. Q.; Cai, C. X.; Ren, X. M.; Duan, C, Y.; Xu, Y.; Gao, S.; You, X. Z. *Chem.—Eur. J.* **2003**, *9*, 5673.
(9) (a) Wang, X.-Y.; Wang, L.; wang, Z.-M.; Su, G.; Gao, S. *Chem. Mater.* **2005**, *17*, 6369–6380. (b) Yang, C.; Wang, Q.-L.; Ma, Y.; Tang, G.-T.; Liao, D.-Z.; Yan, S.-P.; Yang, G.-M.; Peng Cheng, P. *Inorg. Chem.* **2010**, *49*, 2047–2056.

Published on Web 06/02/2010

details of the spin alignments in the AF state.[4,7,9] A number of low-dimensional coordination polymer metal−azido networks have been reported, some of which exhibit long-range ordering behaviors such as ferromagnetism,[10] metamagnetism,[11,12] and weak ferromagnetism.[12,13] Much research has shown the simultaneous presence of both spin-canting and metamagnetism.[7,8]

With regard to the factors that affect magnetic exchange pathways between paramagnetic centers, the proper choice of bridging ligands is of importance since they influence the magnetic strength and behavior of the molecules.[14] Among the most widely used short bridges (such as CN^-, N_3^-, $C_2O_4^{2-}$, $N(CN)_2^-$, etc.), azide is a very important one, because its diverse binding modes lead to variations in the magnetic properties that depend on its orientation with respect to the magnetic centers.[15] To date, the azido ligand has been found to bridge metal ions in the modes of $\mu_{1,1}$-(end-on, EO),[16] $\mu_{1,3}$-(end-to-end, EE),[17] $\mu_{1,1,3}$,[18] $\mu_{1,1,1}$,[19] $\mu_{1,1,1,1}$,[20] $\mu_{1,1,3,3}$,[21] or unusual $\mu_{1,1,1,3,3,3}$ fashions.[22] In general, the end-on mode gives a ferromagnetic interaction, and the end-to-end mode produces antiferromagnetic coupling with exceptional examples.[14,23] Azido-bridged Mn^{III} compounds have evoked much attention mainly for the understanding of the interaction between magnetic centers and for the development of new molecule-based magnets, but only a few have

Scheme 1. (Left) Hphox = 2-(4,5-Dihydrooxazol-2-yl)phenol and (right) HEtphox = 2-(4-Ethyl-4,5-dihydrooxazol-2-yl)phenol

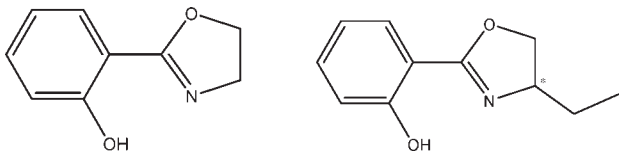

unique features.[24] The larger pseudohalide ligands such as dicyanamide (dca, $N(CN)_2^-$) have also been attracting a lot of attention, partly due to the discovery of long-range magnetic ordering in the α-$M(dca)_2$ compounds.[5b,25,26] It has been shown that this ligand may induce a large variety of topologies and magnetic properties due to its versatile coordination modes.[27−30] In comparison to azido bridging ligands, dca can coordinate metal ions through its eight different kinds of coordination modes. The end-to-end $\mu_{1,5}$ bridging mode of dca with metal ions often gives rise to a weak antiferromagnetic coupling.

There has been increasing interest in the chemistry of oxazoline-based ligands due to their use as chirality-transfer auxiliaries in combination with several transition metals in a wide range of asymmetric catalytic reactions.[31] The stability of the ligands has been proposed to be higher than the salen-type ligands as the oxazoline ring is more stable toward oxidative attack and against hydrolysis.[32] Several metal complexes based on oxazolines have been reported in the literature.[33] The design and synthesis of new chiral oxazoline ligands and their complexes have inspired many scientists to work with great effort.[34] To the best of our knowledge, the presence of magnetic character has not yet been shown for

(10) Shen, Z.; Zuo, J.-L.; Gao, S.; Song, Y.; Che, C.-M.; Fun, H.-K.; You, X.-Z. *Angew. Chem., Int. Ed.* **2000**, *39*, 3633.
(11) Monfort, M.; Resino, I.; Ribas, J.; Stoeckli-Evans, H. *Angew. Chem., Int. Ed.* **2000**, *39*, 191.
(12) (a) Gao, E.-Q.; Bai, S.-Q.; Wang, Z.-M.; Yan, C.-H. *J. Am. Chem. Soc.* **2003**, *125*, 4984. (b) Escuer, A.; Cano, J.; Goher, M. A. S.; Journaux, Y.; Lloret, F.; Mautner, F. A.; Vicente, R. *Inorg. Chem.* **2000**, *39*, 4688.
(13) (a) Escuer, A.; Vicente, R.; Goher, M. A. S.; Mautner, F. A. *Inorg. Chem.* **1995**, *34*, 5707. (b) Escuer, A.; Vicente, R.; Goher, M. A. S.; Mautner, F. A. *Inorg. Chem.* **1997**, *36*, 3440.
(14) Chang, S. H.; Youngkyu, D. *Angew. Chem., Int. Ed.* **1999**, *38*, 193.
(15) Ribas, J.; Monfort, M.; Resino, I.; Solans, X.; Rabu, P.; Maingot, F.; Drillon, M. *Angew. Chem.* **1996**, *108*, 2671. *Angew. Chem., Int. Ed. Engl.* **1996**, *35*, 2520.
(16) (a) Koner, S.; Saha, S.; Mallah, T.; Okamoto, K.-I. *Inorg. Chem.* **2004**, *43*, 840. (b) Song, Y.; Massera, C.; Roubeau, O.; Gamez, P.; Lanfredi, A. M. M.; Reedijk, J. *Inorg. Chem.* **2004**, *43*, 6842. (c) Liu, C.-M.; Yu, Z.; Xiong, R.-G.; Liu, K.; You, X.-Z. *Inorg. Chem. Commun.* **1999**, *2*, 31.
(17) (a) Domínguez-Vera, J. M.; Suárez-Varela, J.; Maimoun, I. B.; Colacio, E. *Eur. J. Inorg. Chem.* **2005**, 1907. (b) Monfort, M.; Resino, I.; Ribas, J.; Solans, X.; Font-Bardia, M.; Stoeckli-Evans, H. *New J. Chem.* **2002**, *26*, 1601. (c) Murugesu, M.; Habrych, M.; Wernsdorfer, W.; Abboud, K. A.; Christou, G. *J. Am. Chem. Soc.* **2004**, *126*, 4766.
(18) (a) Meyer, F.; Demeshko, S.; Leibeling, G.; Kersting, B.; Kaifer, E.; Pritzkow, H. *Chem.s Eur. J.* **2005**, *11*, 1518. (b) Ghoshal, D.; Maji, T. K.; Zangrando, E.; Mallah, T.; Rivière, E. Ä .; Chaudhuri, N. R. *Inorg. Chim. Acta* **2004**, *357*, 1031.
(19) (a) Halcrow, M. A.; Sun, J. S.; Huffman, J. C.; Christou, G. *Inorg. Chem.* **1995**, *34*, 4167. (b) Karmakar, T. K.; Chandra, S. K.; Ribas, J.; Mostafa, G.; Lu, T. H.; Ghosh, B. K. *Chem. Commun.* **2002**, 2364.(c) Zhang, L.; Tang, L.-F.; Wang, Z.-H.; Du, M.; Julve, M.; Lloret, F.; Wang, J.-T. *Inorg. Chem.* **2001**, *40*, 3619. (d) Ma, D.-Q.; Hikichi, S.; Akita, M.; Moro-oka, Y. *J. Chem. Soc., Dalton Trans.* **2000**, 1123. (e) Goher, M. A. S.; Cano, J.; Journaux, Y.; Abu-Youssef, M. A. M.; Mautner, F. A.; Escuer, A.; Vicente, R. *Chem.—Eur. J.* **2000**, *6*, 778.
(20) (a) Papaefstathiou, G. S.; Perlepes, S. P.; Escuer, A.; Vicente, R.; Font-Bardia, M.; Solans, X. *Angew. Chem., Int. Ed.* **2001**, *40*, 884. (b) Papaefstathiou, G. S.; Escuer, A.; Vicente, R.; Font-Bardia, M.; Solans, X.; Perlepes, S. P. *Chem. Commun.* **2001**, *23*, 2414.
(21) (a) Demeshko, S.; Leibeling, G.; Maringgele, W.; Meyer, F.; Mennerich, C.; Klauss, H.-H.; Pritzkow, H. *Inorg. Chem.* **2005**, *44*, 519. (b) Meyer, F.; Kircher, P.; Pritzkow, H. *Chem. Commun.* **2003**, *6*, 774.
(22) (a) Mialane, P.; Dolbecq, A.; Marrot, J.; Rivière, E.; Sécheresse, F. *Chem.—Eur. J.* **2005**, *11*, 1771.
(23) (a) Hong, C. S.; Koo, J.-e.; Son, S.-K.; Lee, Y. S.; Kim, Y.-S.; Do, Y. *Chem.—Eur. J.* **2001**, *7*, 4243. (b) You, Y. S.; Hong, C. S.; Kim, K. M. *Polyhedron* **2005**, *24*, 249.
(24) (a) Ribas, J.; Escuer, A.; Monfort, M.; Vicente, R.; Cortés, R.; Lezama,L.; Rojo, T. *Coord. Chem. Rev.* **1999**, *193−195*, 1027 and references cited therein. (b) Reddy, K. R.; Rajasekharan, M. V.; Tuchagues, J.-P. *Inorg. Chem.* **1998**, *37*, 5978. (c) Li, H.; Zhong, Z. J.; Duan, C.-Y.; You, X.-Z.; Mak, T. C. W.; Wu, B. *Inorg. Chim. Acta* **1998**, *271*, 99. (d) Panja, A.; Shaikh, N.; Vojtisek, P.; Gao, S.; Banerjee, P. *New J. Chem.* **2002**, *26*, 1025. (e) Stults, B. R.; Marianelli, R. S.; Day, V. W. *Inorg. Chem.* **1975**, *14*, 722.
(25) Batten, S. R.; Jensen, P.; Moubaraki, B.; Murray, K. S.; Robson, R. *Chem. Commun.* **1998**, *3*, 439.
(26) Manson, J. L.; Kmety, C. R.; Huang, Q.-z.; Lynn, J. W.; Bendele, G. M.; Pagola, S.; Stephens, P. W.; Liable-Sands, L. M.; Rheingold, A. L.; Epstein, A. J.; Miller, J. S. *Chem. Mater.* **1998**, *10*, 2552.
(27) Dasna, I.; Golhen, S.; Ouahab, L.; Daro, N.; Sutter, J.-P. *New J. Chem.* **2001**, *25*, 1572.
(28) Batten, S. R.; Jensen, P.; Moubaraki, B.; Murray, K. S.; Robson, R. *Chem. Commun.* **1998**, *3*, 439.
(29) Kurmoo, M.; Kepert, C. J. *New J. Chem.* **1998**, *22*, 1515.
(30) Jensen, P.; Batten, S. R.; Moubaraki, B.; Murray, K. S. *Chem. Commun.* **2000**, *9*, 793.
(31) (a) Rechavi, D.; Lemaire, M. *Chem. Rev.* **2002**, *102*, 3467. (b) Johnson, J. S.; Evans, D. A. *Acc. Chem. Res.* **2000**, *33*, 325. (c) Pfaltz, A. *Acc. Chem. Res.* **1993**, *26*, 339. (d) Ghosh, A. K.; Mathivanan, P.; Cappiello, J. *Tetrahedron: Asymmetry* **1998**, *9*, 1. (e) Bolm, C.; Bienewald, F.; Schlingloft, G. *J. Mol. Catal.* **1997**, *117*, 347. (f) Bolm, C.; Bienewald, F.; Harms, K. *Synlett.* **1996**, 775. (g) Bolm, C.; Bienewald, F. *Angew. Chem., Int. Ed. Engl.* **1995**, *34*, 2640. (h) Moreno, R. M.; Bueno, A.; Moyano, A. *J. Organomet. Chem.* **2003**, *671*, 187.
(32) (a) Godbole, M. D.; Hotze, A. C. G.; Hage, R.; Mills, A. M.; Kooijman, H.; Spek, A. L.; Bouwman, E. *Inorg. Chem.* **2005**, *44*, 9253. (b) Stefano, C.; Dominique, S. *J. Comb. Chem.* **2005**, *7*, 688.
(33) You, Y. S.; Yoon, J. H.; Kim, H. C.; Hong, C. S. *Chem. Commun.* **2005**, *32*, 4116.
(34) (a) Ghoshal, S.; Wadawale, A.; Jain, V. K.; Nethaji, M. *J. Chem. Res.* **2007**, *4*, 221. (b) Kandasamy, K.; Singh, H. B.; Butcher, R. J.; Jasinski, J. P. *Inorg. Chem.* **2004**, *43*, 5704. (c) Zhao, W.; Qian, Y.-L.; Huang, J.; Duan, J. *J. Organomet. Chem.* **2004**, *689*, 2614. (d) Zhang, Y.; Kong, D.; Liu, T.-F.; Xu, W. G. *Acta Crystallogr., Sect. E* **2007**, *63*, m1396. (e) Zhang, Y.; Kong, D.; Liu, T.-F.; Xu, W. G. *Acta Crystallogr., Sect. E* **2007**, *63*, m2292. (f) Zhang, Y.; Kong, D.; Liu, T.-F.; Xu, W. G. *Acta Crystallogr., Sect. E* **2007**, *63*, m2231.

azide-bridged and dca-bridged Mn(III) systems with the Hphox and HEtphox ligands.

Herein, we report the synthesis, crystal structures, and magnetic properties of three one-dimensional chains, $[Mn(phox)(N_3)]_n$(**1**), $[Mn(Etphox)(N_3)]_n$(**2**), and $[Mn(Etphox)_2(C_2N_3)]_n$ (**3**), using oxazoline-based ligands linked by azide or dicyanamide in a single end-to-end fashion, where achiral ligand Hphox is 2-(4,5-dihydrooxazol-2-yl)phenol (Scheme 1a) and chiral ligand HEtphox is 2-(4-ethyl-4,5-dihydrooxazol-2-yl)phenol) (Scheme 1b). All complexes are similar in local coordination environments but somewhat different in bridging parameters. All the complexes are of one-dimensional chain structures and form 2D frameworks by weak interactions. The adjacent 1D chains of complex **1** are connected by face-to-face $\pi-\pi$ interactions, $C-H\cdots\pi$ interactions, and hydrogen bonding, which leads to the formation of a supramolecular 2D sheet structure. Only hydrogen bonding can be found in complex **2** and only $C-H\cdots\pi$ interactions in complex **3** because of the existence of substituents. Therefore, they should be appropriate for magnetostructural studies. Both compounds **1** and **3** show antiferromagnetic coupling between Mn^{III} ions but no long-range ordering above 2 K. Compound **2** shows the concomitant existence of spin canting and metamagnetism below 10 K, and metamagnetic behavior reveals a two-step magnetic phase transition, which is a unique example of the one-dimensional Mn(III) systems connected by end-to-end azide ligands.

Experimental Section

Materials and Instrumentation. All chemicals and solvents were commercially available reagents of analytical grade and used as received without further purification. The achiral ligand Hphox was prepared from 2-hydroxybenzonitrile and ethanolamine using the modified published procedure.[35,36] The racemic ligand HEtphox was prepared by a method similar to that of Hphox by using 2-hydroxybenzonitrile and racemic 2-aminobutanol. All preparations and manipulations were performed under aerobic conditions. The infrared spectra were recorded against pure crystals on a Nicolet 170SXTF/IR spectrometer in the range 4000−400 cm^{-1}.

X-Ray Crystallography. A single crystal with approximate dimensions was used for X-ray diffraction analysis. Determination of the unit cell and data collection were performed on a Bruker SMART 1000X diffractometer using graphite monochromated Mo K_α radiation. The structure was solved by direct methods in SHELXS-97[37] and refined using a full-matrix least-squares procedure on F^2 in SHELXS-97.[38] The disordered C13 sites of compounds **2** were refined with an equal occupation factor of 0.5.

Magnetic Measurements. Magnetic data were recorded using a Quantum Design SQUID magnetometer. The isothermal magnetizations were measured with an applied field from −50 to +50 kOe. The ac measurements were performed at various frequencies from 1 to 1000 Hz with an ac field amplitude of 3 Oe under zero dc field. To avoid orientation in the magnetic field, the samples were pressed in a homemade Teflon sample holder equipped with a piston. The data were corrected for diamagnetism of the constituent atoms using Pascal's constants.

Table 1. Crystallographic Data for the Complexes **1**, **2**, and **3**

compound	**1**	**2**	**3**
formula	$C_{18}H_{16}MnN_5O_4$	$C_{22}H_{24}MnN_5O_4$	$C_{24}H_{24}MnN_5O_4$
M_r [g mol^{-1}]	421.30	477.40	501.42
T [K]	296(2)	295(2)	293(2)
λ [Å]	0.71073	0.71073	0.71073
cryst syst	triclinic	triclinic	monoclinic
space group	$P\bar{1}$	$P\bar{1}$	$P2_1/n$
a [Å]	6.336(3)	10.050(5)	8.7927(18)
b [Å]	6.646(3)	10.525(6)	11.472(2)
c [Å]	11.911(6)	11.158(6)	12.010(2)
α [deg]	80.023(7)	96.949(9)	90
β [deg]	82.159(7)	103.657(9)	106.37(3)
γ [deg]	62.717(6)	99.462(9)	90
V [$Å^3$]	438.0(4)	1115.4(10)	1162.4(4)
Z	1	2	2
ρ_{calcd} [g cm^{-3}]	1.597	1.422	1.433
μ [mm^{-1}]	0.791	0.630	0.609
$F(000)$	216	496	520
cryst size [mm]	0.24 × 0.18 × 0.15	0.28 × 0.14 × 0.11	0.33 × 0.30 × 0.27
θ [deg]	1.74- 28.42	1.90 - 28.66	3.11- 27.48
measured reflns	2759	6351	9299
unique refln	1988	3795	2644
R(int.)	0.0141	0.0701	0.0428
data/restaints/ params	1988/0/130	3795/0/294	2644/0/171
GOF on F^2	1.089	0.835	1.150
R_1 [$I > 2\sigma(I)$]	0.0301	0.0775	0.0639
wR_2 [$I > 2\sigma(I)$]	0.0829	0.1645	0.1559
R_1 (all data)[a]	0.0315	0.1021	0.0703
wR_2 (all data)[b]	0.0841	0.1735	0.1605
largest diff. peak and hole [$eÅ^{-3}$]	0.248, −0.389	0.566, −0.618	0.543,-0.674

[a] $R_1 = \sum||F_o| - |F_c||/\sum|Fo|$. [b] $wR_2 = \sum[w > (F_o^2 - F_c^2)^2]/\sum[w > (F_o^2)^2]^{1/2}$.

Caution! *Azide compounds are potentially explosive! Only a small amount of material should be prepared and handled with care.*

Catena-$[Mn(phox)_2(N_3)]$ (1). This complex was synthesized by mixing a solution of Hphox (0.16 mmol) in methanol (1.60 mL) with a solution of $Mn(CH_3COO)_2\cdot 4H_2O$ (49.02 mg, 0.2 mmol) in methanol (2.00 mL), followed by the dropwise addition of an aqueous solution (2.00 mL) of NaN_3 (13 mg, 0.2 mmol) without stirring. The dark-green mixture was allowed to stand for several days until good-quality dark-green diamond crystals of complex **1** were obtained in a yield of 58.3%. Anal. Calcd for $C_{18}H_{16}MnN_5O_4$: C, 51.3; H, 3.8; N, 16.6%. Found: C, 51.4; H, 3.8; N, 16.4%. IR spectrum (KBr pellet, cm^{-1}): 438.16 w, 570.91 m, 645.41 w, 673.59 s, 684.82 m, 748.82 s, 863.44 vs, 931.81 s, 1079.16 s, 1032.97 w, 1143.03 m, 1156.92 m, 1248.58 vs, 1333,54 m, 1397.13 m, 1441.90 m, 1472.98 br, 1546.03 m, 1591.81 br, 1623.92 vs, 2055.75 s, 2346.07 br, 2370.15 br, 3448.44 m.

Catena-$[Mn(Etphox)_2(N_3)]$ (2). In a test tube, an aqueous solution (2.00 mL) of NaN_3 (13 mg, 0.2 mmol) was layered carefully. And then a mixture made by a methanol solution of HEtphox (0.16 mmol, 1.60 mL) and a methanol solution of $Mn(CH_3COO)_2\cdot 4H_2O$ (0.2 mmol, 2.00 mL) was added. The tube was sealed and left undisturbed at room temperature. After several days, good-quality dark-green needle crystals of complex **2** were obtained in a yield of 61.9%. Anal. Calcd for $C_{22}H_{24}MnN_5O_4$: C, 55.3; H, 5.0; N, 14.7%. Found: C, 55.5; H, 5.1; N, 14.4%. IR spectrum (KBr pellet, cm^{-1}): 418.07 m, 454.34 w, 575.71 w, 645.08 w, 668.47 m, 687.99 m, 752.67 s, 862.39 vs, 927.20 m, 941.18 m, 976.76 w, 1032.76 m, 1078.26 s, 1147.04 br, 1158.74 s, 1241.83 vs, 1256.06 br, 1258.00 w, 1326.92 vs, 1397.41 vs, 1444.77 s, 1497.40 vs, 1549.70 s, 1590.55 s, 1611.76 vs, 2017.17 br, 2038.49 vs, 2916.13 w, 2958.89 br, 2972.90 br, 3029.16 br, 3055.47 br, 3363.95 w.

(35) Jose, L. S.; Teresa, S.; Yolanda, G.; Carsten, B.; Konrad, W.; Angelika, M.; Guido, M. *J. Am. Chem. Soc.* **1995**, *117*, 8312.
(36) Cozzi, P. G.; Floriani, C.; Chiesi-V., A.; Rizzoli, C. *Inorg. Chem.* **1995**, *34*, 2921.
(37) Sheldrick, G. M. *SHELXS-97*; University of Gottingen: Gottingen, Germany, 1990.
(38) Sheldrick, G. M. *SHELXS-97*; University of Gottingen: Gottingen, Germany, 1997.

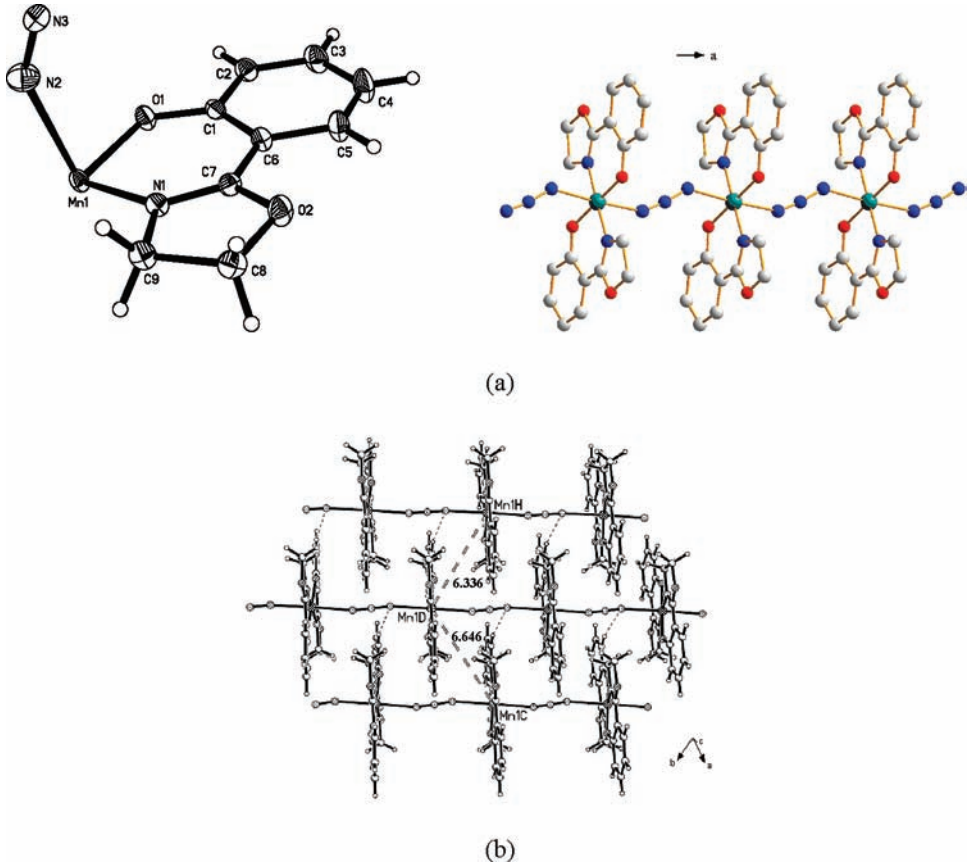

Figure 1. (a) The molecular structure (30% thermal probability ellipsoids) of complex **1** showing the atom numbering. The chain of **1** is running along the *a* axis. (b) Formation of a sheet by the locking of 1D $[Mn(phox)_2(N_3)]_n$ chains with face-to-face $\pi-\pi$ interactions, $C-H\cdots\pi$ interactions, and hydrogen bonding between the neighboring chains.

Catena- [Mn(Etphox)$_2$(C_2N_3)] (3). This complex was synthesized in the same way as **2**, using an aqueous solution (2.00 mL) of NaC_2N_3 (17.8 mg,0.2 mmol) instead of NaN_3 and a solution of $MnCl_2\cdot4H_2O$ (36.0 mg, 0.2 mmol) in methanol (2.00 mL) instead of $Mn(CH_3COO)_2\cdot4H_2O$. The dark-green mixture was allowed to stand for several days until good-quality dark-green needle crystals were obtained in a yield of 65.6%. Anal. Calcd for $C_{24}H_{24}MnN_5O_4$: C, 57.4; H, 4.8; N, 14.0%. Found: C, 57.5; H, 4.7; N, 14.2%. IR spectrum (KBr pellet, cm^{-1}): 437.71 m, 506.06 w, 574.28 w, 646.32 w, 674.13 m, 759.77 s, 867.99 br, 940.80 br, 1030.71 w, 1077.45 m, 1141.47 m, 1157.58 m, 1238.50 s, 1260.03 s, 1331.96 s, 1374.01 m, 1400.80 s, 1444.82 m, 1461.17 w, 1480.79 s, 1550.20 m, 1591.22 m, 1613.72 vs, 2156.67 vs, 2224.51 w, 2294.04 m, 2871.38 w, 2927.63 br, 2968.95 br, 3056.69 w.

Results and Discussion

Structures. Single-crystal X-ray diffraction of **1** reveals that it crystallizes in the triclinic space group $P\bar{1}$, and the structure is presented in Table 1. The structure of the molecular unit is shown in Figure 1a, and the selected bonds and angles are shown in Table 2. The Mn center has a distorted octahedral arrangement consisting of two O atoms from the ligand and four N atoms from the ligand and the azido bridges. A significant elongation around the Mn(III) ion occurs as a result of the Jahn−Teller effect. The two axial sites are separated from Mn1 with 2.360(2) Å for Mn1−N2 and Mn(1)−N(2)$^{\#1}$, much longer than the equatorial plane average Mn−N(O) distance of 1.92(3) Å. Mn−azide geometric data pertinent to the magnetic properties are N3−N2−Mn1 = 144.23(13)°. The cationic units are linked together through the azide ligands in *trans*-positions, resulting in a one-dimensional chain with single azido bridges coordinated in the EE mode along the crystallographic *a* axis. The Mn−azido−Mn torsion angle, defined by the dihedral angle between the mean planes of Mn1−N_3−Mn2, is 2.954(9)°, indicating that they almost lie in the same plane. The shortest intra- and interchain Mn−Mn distances are 6.760(3) and 6.336(4) Å, respectively.

Table 2. Selected Bond Lengths (Å) and Angles (deg) for Compound **1**[a]

Mn1−O1	1.871(1)	Mn1−N1#1	1.994(1)
Mn1−O1#1	1.871(1)	Mn1−N2#1	2.360(2)
Mn1−N1	1.994(1)	Mn1−N2	2.360(2)
N2−N3	1.171(2)	N3−N2#2	1.171(2)
N1#2−N3-N2	173.4(1)	N1−Mn1−N2#1	88.66(6)
O1−Mn1−N1	89.99(6)	N1#1−Mn1-N2	88.66(6)
O1#1−Mn1-N1	90.01(6)	O1−Mn1−N2	91.62(7)
O1−Mn1−N1#1	90.01(6)	O1#1−Mn1-N2	88.38(7)
N3−N2−Mn1	144.23(13)	N1−Mn1−N2	91.34(6)
O1−Mn1−N2#1	88.38(7)		

[a] Symmetry operation: #1 $-x+1, -y+1, -z+1$. #2 $-x+2, -y, -z+1$.

The crystal packing of **1** indicates that the adjacent 1D chain orients the oxazoline ligand in such a way that the chains are interlocked by face-to-face $\pi-\pi$ interactions. One part of the interactions occurs between the oxazoline rings [R1 = C7−O2−C8−C9−N1] and benzol rings [R2 = C1 to C6], having there centroid−centroid distances of 3.875(6) Å. The dihedral angles between the rings are 4.773(2)°. The

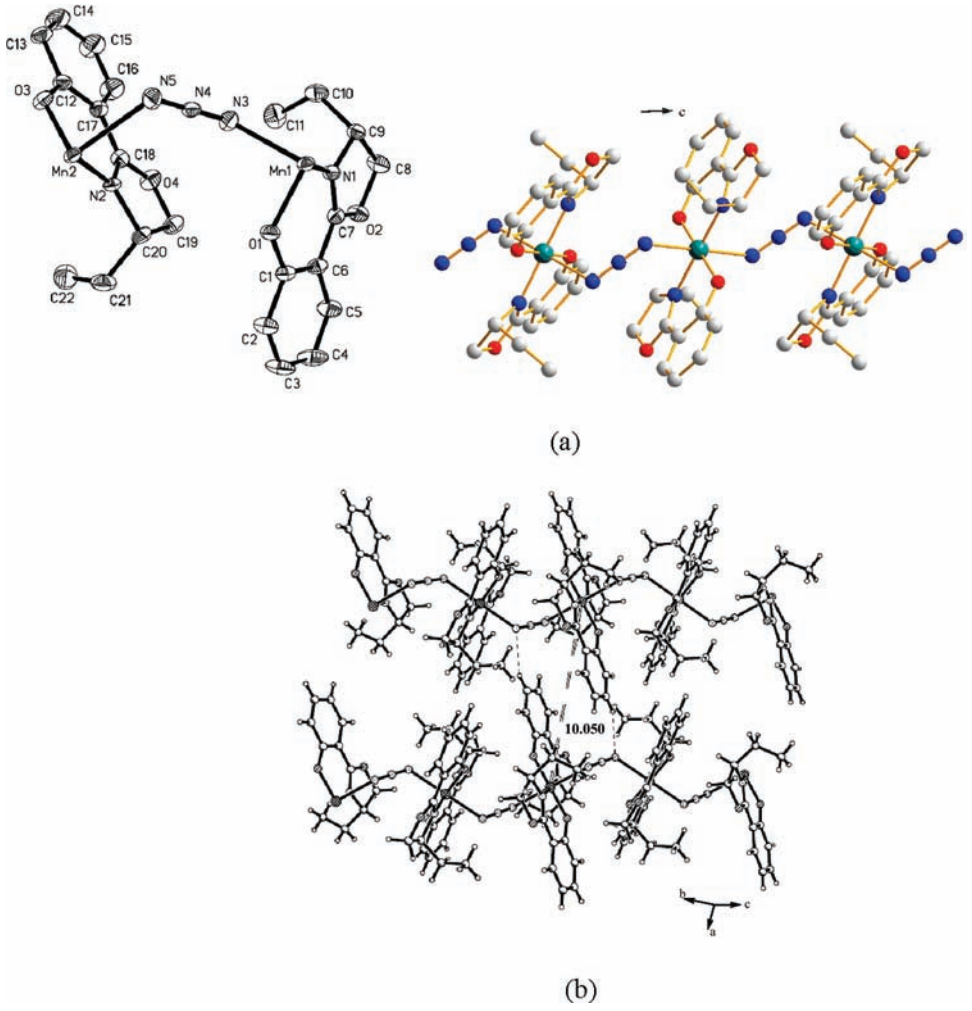

Figure 2. (a) Molecular structure (30% thermal probability ellipsoids) of complex **2** showing the atom numbering (hydrogen atoms are omitted for clarity). The chain of **2** is running along the *c* axis. (b) The hydrogen bonding between the neighboring chains (dotted lines).

$\pi-\pi$ interactions are supplemented by the C−H···π interactions [C8−H8A and C8−H8B] to the ring R4 with an H···R average distance of 2.610(5) Å and a C−H···π average angle of 153° to form a supramolecular 2D sheet (Figure 1b). Weak interchain C2−H2···N2 hydrogen bonds between adjacent chains also contribute to the 2D framework. The distance C2···N2 is 3.514(3) Å, and the hydrogen bond angle ∠C2−H2···N2 is 166°.

The crystal structure of **2** is also built up from oxazoline-based ligands and azido-bridged Mn ions (Figure 2; Table 3). Each Mn^{III} ion has a slightly distorted octahedral coordination, formed by two nitrogen atoms and two oxygen atoms from the oxazoline-based ligands and two nitrogen atoms from the bridges. The equatorial N_2O_2 plane originating from the ligands exhibits an average Mn−N(O) distance of 1.94(6) Å, while the remaining two axial sites are separated by 2.278(4) Å for Mn1−N3 and 2.316(1) Å for Mn2−N5. Mn−azide geometric data pertinent to the magnetic properties are N4−N3−Mn1, 120.54(26)°; N3−N4−N5, 179.2(4)°; N3−N4, 1.188(5) Å. The dihedral angle of Mn1−N_3−Mn2 is 76.47(22)°. Another structural feature of **2** manifests itself in the difference in arrangement of the two adjacent centrosymmetric units. The phenyl rings are arranged alternately with their faces parallel to each other along the *c* axis. The shortest intra- and interchain Mn−Mn distances are 5.579(3) and 10.050(5) Å, respectively. The bigger dihedral angle and the longer distance between neighboring chains are both the result of ethyl's existence. No clear $\pi-\pi$ interactions are found between chains. The adjacent chains are interlocked by interchain C14−H14···N3 hydrogen bonds. The distance C14···N3 is 3.480(5) Å, a little longer than that of **1**. The hydrogen bond angle ∠C14−H14···N3 is 159°.

Table 3. Selected Bond Lengths (Å) and Angles (deg) for Compound **2**[a]

Mn1−O1	1.882(3)	Mn1−O1	1.882(3)
Mn1−N1	2.010(4)	Mn1−N1#1	2.010(4)
Mn1−N3	2.279(4)	Mn1−N3#1	2.279(4)
Mn2−O3	1.865(3)	Mn2−O3#2	1.865(3)
Mn2−N2	2.004(4)	Mn2−N2#2	2.004(4)
Mn2−N5	2.316(4)	Mn2−N5#2	2.316(4)
N3−N4	1.188(5)		
O1#1−Mn1−N1	91.12(14)	O1−Mn1−N1#1	91.12(14)
O1−Mn1−N3#1	89.49(14)	O1−Mn1−N1	88.88(14)
O1#1−Mn1−N3	89.49(14)	N1−Mn1−N3#1	87.11(14)
O1−Mn1−N3	90.51(14)	N1−Mn1−N3	92.89(14)
N1#1−Mn1−N3	87.11(14)	N5−N4−N3	179.2(4)
O3−Mn2−N5	89.10(15)	O3−Mn2−N2#2	90.09(13)
O3#2−Mn2−N2	90.09(13)	O3−Mn2−N2	89.91(13)
N2−Mn2−N5	87.08(14)	N2#2−Mn2-N5	92.92(14)
O3−Mn2−N5#2	90.90(15)	N4−N3−Mn1	120.5(3)
N2−Mn2−N5#2	92.92(14)	O3#2−Mn2-N5	90.90(15)

[a] Symmetry operation: #1 $-x+1, -y, -z+1$. #2 $-x+1, -y, -z$.

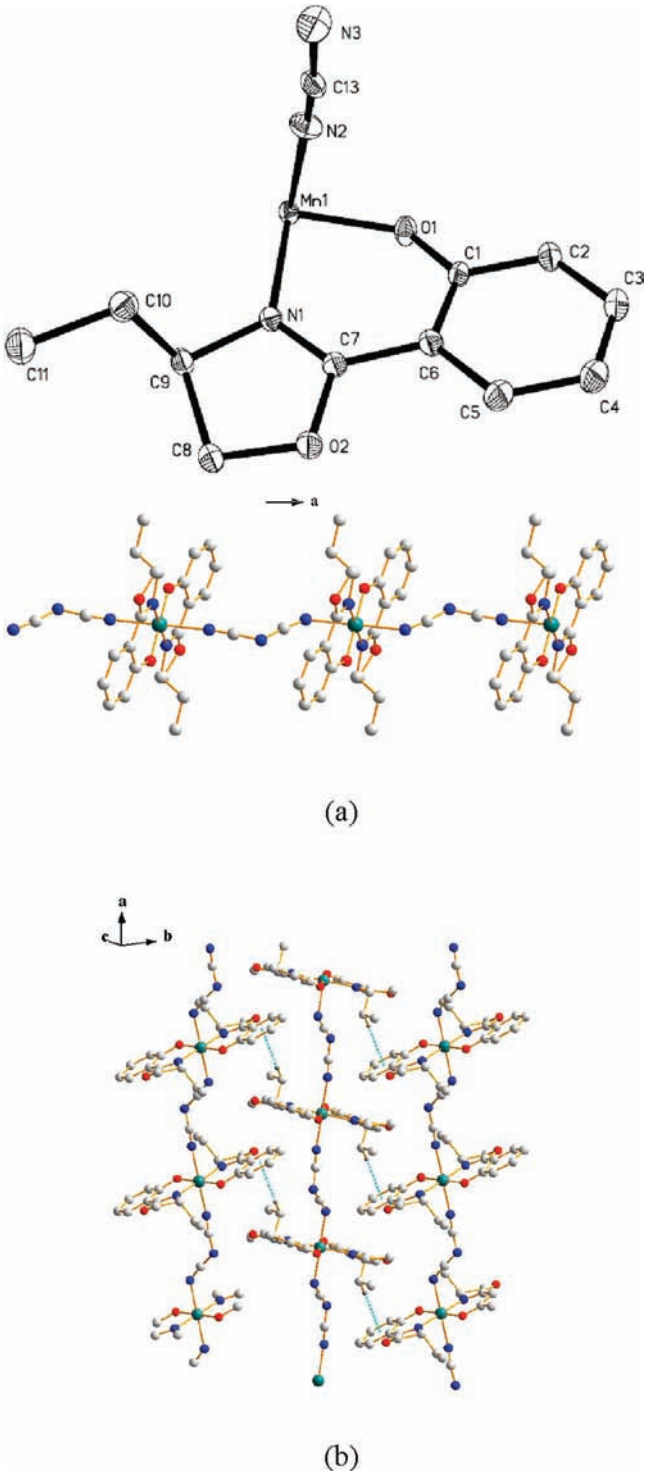

Figure 3. (a) Molecular structure (30% thermal probability ellipsoids) of complex **3** showing the atom numbering (hydrogen atoms are omitted for clarity). Only one position of disorder atom C13 is shown. The chain is running along the *a* axis. (b) Formation of a sheet by the locking of 1D $[Mn(Etphox)_2(C_2N_3)]_n$ chains through C−H···π interactions (dotted magenta lines). H atoms (except the CH− forming C−H···π interactions) are omitted for clarity.

Complex **3** crystallizes in the triclinic space group $P2_1/n$, and the structure is presented in Table 1. The molecular structure is presented in Figure 3. Selected bond lengths and angles are given in Table 4. The geometry around the manganese centers could also be described as a distorted

Table 4. Selected Bond Lengths (Å) and Angles (deg) for Compound **3**[a]

Mn1−O1#1	1.860(2)	Mn1−O1	1.860(2)
Mn1−N1	2.019(3)	Mn1−N1#1	2.019(3)
Mn1−N2#1	2.276(3)	Mn1−N2	2.276(3)
O1−Mn1−N1	89.60(11)	O1−Mn1−N2	87.33(13)
O1−Mn1−N1#1	90.40(11)	O1#1−Mn1−N1	90.40(11)
O1#1−Mn1−N2	92.67(13)	O1−Mn1−N2#1	92.67(13)
N1−Mn1−N2#1	92.02(12)	N1−Mn1−N2	87.98(12)
N1#1−Mn1−N2	92.02(12)		

[a] Symmetry operation: #1: $-x, -y+1, -z+1$. #2 $-x+1, -y+1, -z+1$.

octahedral with the basal planes defined by two nitrogen atoms and two oxygen atoms of the coordinated ligands and two terminal nitrogen atoms of the bridging dca ligand. The coordinated nitrogen atoms of the dca ligands occupy the apical positions (N2 and N2a; symmetry operation: $-x, -y+1, -z+1$) with 2.276(6) Å for Mn1−N2 (Mn1−N2a). The equatorial N_2O_2 plane originating from the ligand exhibits an average Mn−N(O) distance of 1.93(9) Å. The crystal structure is characterized by $[Mn(Etphox)_2(\mu_{1,5}\text{-dca})]$ units linked into 1D polymeric chains where the dca anion connects the manganese(III) ion of the symmetry related unit in an end-to-end bridging mode. The chains propagate parallel to the crystallographic *a* axis. The shortest intra- and interchain Mn−Mn distances are 8.792(7) and 8.567(9) Å, respectively, which are rather long to have effective magnetic coupling. The dicyanamide ligands are bent, with the $C13-N3-C13^{\#1}$ angle around 125° and two straight linear units with angles ∠N2−C13−N3 = 174.1° and ∠N3−C13a−N2a = 173.6°. The dihedral angel of Mn1−C_2N_3−Mn2 is 0.87(9)°, which is the smallest one among the three complexes. No clear $\pi-\pi$ interactions are found in complex **3**. But the compound forms a supramolecular 2D sheet by C−H···π interactions [C10−H10B to the ring R (R = C1, C2, C3, C4, C5, C6)] with a H···R distance of 2.740 Å and a C−H···π angle of 162°.

The phenomena above may be explained by the fact that packing arrangements of aromatic hydrocarbons depend on the number and positioning of C and H atoms in a molecule.[39] The lack of substituents, which strongly affect electron distribution or enable strong hydrogen-bond formation, makes possible the prediction of crystal packing of simple aromatic hydrocarbons. And in some situations, substitution(s) of the aromatic system may exclude stacking completely.[40]

Magnetic Measurements

The magnetic susceptibilities of complexes **1** and **3**, shown in Figure 4, were measured at 0.1 T in the temperature range 5.0−300 K for **1** and 2.0−300 K for **3**. They exhibit similar magnetic properties. The $\chi_M T$ value of 2.76 cm^3 K mol^{-1} for **1** at 300 K is slightly smaller than the expected value for

(39) (a) Desiraju, G. R.; Gavezzotti, A. *Acta Crystallogr.* **1989**, *B45*, 473. (b) Desiraju, G. R.; Gavezzotti, A. *J. Chem Soc., Chem. Commun.* **1989**, *10*, 621. (c) Gavezzotti, A.; Desiraju, G. R. *Acta Crystallogr., Sect. B* **1988**, *44*, 427. (d) Gavezzotti, A. *Chem. Phys. Lett.* **1989**, *161*, 427.

(40) Główka, M. L.; Martynowski, D.; Kozłowska, K. *J. Mol. Struct.* **1999**, *474*, 81.

(41) Wagner, G. R.; Friendberg, S. A. *Phys. Lett.* **1964**, *9*, 11.

(42) (a) Hyun Hee, K; Jeong Hak, L; Hyoung Chan, K; Chang Seop, H. *Inorg. Chem.* **2006**, *45*, 8847. (b) Rajender Reddy, K.; Rajasekharan, M. V.; Tuchagues, J.-P. *Inorg. Chem.* **1998**, *37*, 5978. (c) Kennedy, B. J.; Murray, K. S. *Inorg. Chem.* **1985**, *24*, 1552.

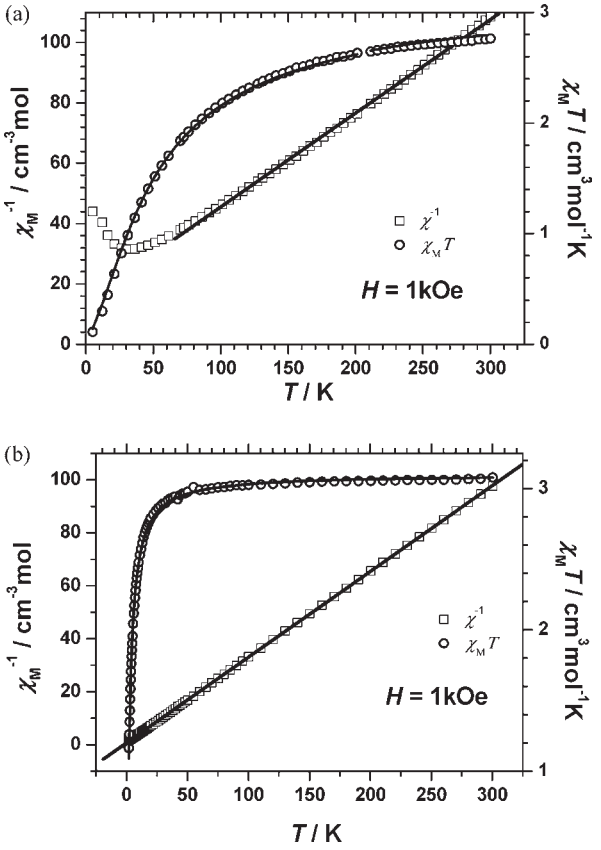

Figure 4. (a) Plot of χ_M^{-1} vs T (□) and $\chi_M T$ vs T (○) for **1**. (b) Plot of χ_M^{-1} vs T (□) and $\chi_M T$ vs T (○) for **3**. The solid line represents the best fit of the experimental data.

noninteracting Mn(III) ions, and the $\chi_M T$ value of 3.08 cm^3 K mol^{-1} for **3** is slightly higher than the expected value. As the temperature is lowered, the $\chi_M T$ value undergoes a gradual decrease down to 0.11 cm^3 K mol^{-1} at 5 K for **1** and 1.16 cm^3 K mol^{-1} at 2 K for **3**, indicating antiferromagnetic couplings between the magnetic centers. The molar susceptiblities of **1** obey the Curie−Weiss law in the high-temperature region 100−300 K, yielding $C = 3.25$ cm^3 K mol^{-1} and $\theta = -48.93$ K. The magnetic susceptibility of **3** obeys the Curie−Weiss law perfectly, as shown, with $C = 3.37$ cm^3 K mol^{-1} and $\theta = -3.71$ K. On the basis of the 1D model, the magnetic susceptibilities can be fitted accordingly by the Fisher infinite-chain model derived from the exchange spin Hamiltonian 1D chain:[43,44]

$$\chi_M = \frac{N\beta^2 g^2}{3kT} S(S+1)\left[\frac{1+U}{1-U}\right]$$

where

$$U = \coth\frac{-2JS(S+1)}{kT} - \frac{-2JS(S+1)}{kT}$$

Fitting of the observed data gave best-fit parameters of $g = 2.06$ and $J = -3.42$ cm^{-1} with $R = 7.46 \times 10^{-5}$ ($R = \sum[(\chi_M)_{obs} - (\chi_M)_{calc}]^2/\sum[(\chi_M)_{obs}]^2$) for **1** and $g = 2.03$ and $J = -0.196$ cm^{-1} with $R = 4.916 \times 10^{-5}$ for **3**. The negative J values demonstrate that Mn(III) spins bridged by end-to-end azides in the chains are coupled antiferromagnetically, which are consistent with azide-bridged Mn(III) systems.[42]

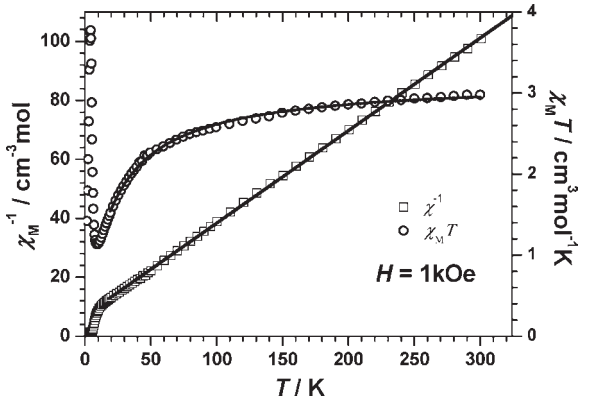

Figure 5. Plot of χ_M^{-1} vs T (□) and $\chi_M T$ vs T (○) for **2**. The solid line shows the best theoretical fit.

It is of great interest to study the magnetic properties of **2** and make a comparison with those of **1** and **3**. The χ_M^{-1} and $\chi_M T$ versus T curves for complex **2** are shown in Figure 5. The magnetic susceptibility was also measured at 0.1 T in the temperature range 2.0−300 K. The $\chi_M T$ value of 2.98 cm^3 K mol^{-1} at room temperature is still slightly smaller than the spin-only value. As the temperature is lowered, $\chi_M T$ undergoes a gradual decrease down to 1.13 cm^3 K mol^{-1} at 10 K, indicating antiferromagnetic couplings.

At low temperatures (< 10 K), the $\chi_M T$ product experiences an upturn, arriving at a maximum 3.77 cm^3 K mol^{-1} at 4.9 K, suggesting a long-range ordering due to the spin-canting below 10 K. Upon further cooling, $\chi_M T$ drops sharply, suggesting AF interactions between the chains or the saturation effect. The cryomagnetic behavior of **2** obeys the Curie−Weiss law in the high-temperature region 100−300 K, yielding $C = 3.15$ cm^3 K mol^{-1} and $\theta = -21.01$ K. The magnetic data above 20 K can be analyzed using an infinite-chain model derived by Fisher.[43,44] A best fit gives parameters of $g = 2.02$ and $J = -1.35$ cm^{-1} with $R = 2.01 \times 10^{-4}$. The negative J value demonstrates that Mn(III) spins bridged by an end-to-end azide in a chain are coupled antiferromagnetically.

To further clarify the magnetic behavior, the temperature dependencies of ac magnetic susceptibility under $H_{dc} = 0$ Oe and $H_{ac} = 3$ Oe were carried out, with frequencies of 10, 100, and 1000 Hz from 2 to 8 K (Figure S1, Supporting Information). The in-phase ac signal presents a peak at 5.6 K, confirming the occurrence of a phase transition, consistent with the temperature dependency data of dc susceptibility. The occurrence of the nonzero out-of-phase signal also indicates the existence of the phase transition. No frequency dependence of the ac signals was observed.

The magnetization versus applied field variations below the transition temperatures are shown in Figure 6. The field-dependent magnetization of complex **2** exhibits a sigmoid shape, which is characteristic of a magnetic transition induced by the external field. The initial increase of magnetization is relatively rapid, and then it becomes almost linear with a smaller slope up to 1.09 per Mn^{3+} at 50 kOe, far from the experimental saturation value of the Mn^{3+} ion, suggesting the overall AF coupling between Mn^{3+} ions. The hysteresis loop for **2** measured at 2 K reveals a two-step magnetic phase

(43) Fisher, M. E. *Am. J. Phys.* **1964**, *32*, 343.
(44) (a) Dzyaloshinsky, I. *J. Phys. Chem. Solids* **1958**, *4*, 241. (b) Moriya, T. *Phys. Rev.* **1960**, *117*, 635; **1960**, *120*, 91. (c) Wang, X.-T.; Wang, X.-H.; Wang, Z. -M.; Gao, S. *Inorg. Chem.* **2009**, *48*, 1301.

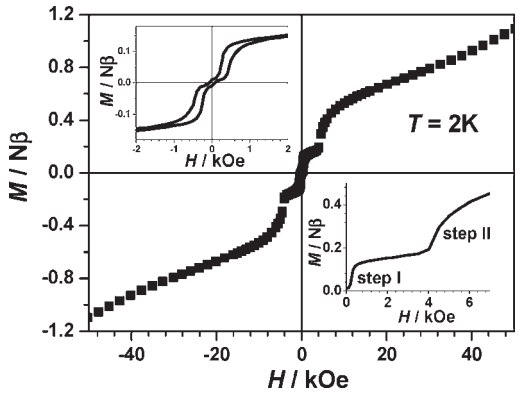

Figure 6. Field dependence of the magnetization of **2**. The inset gives a blown-up view of the hysteresis loop below 2 kOe.

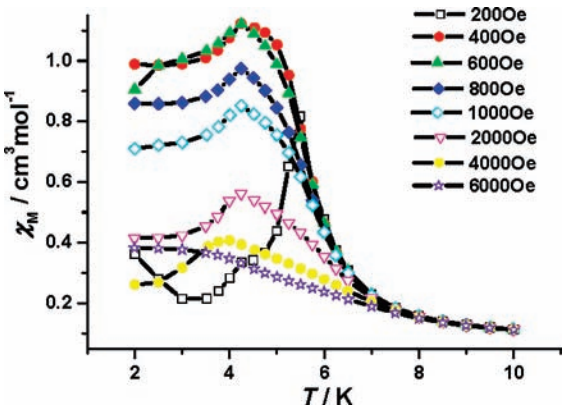

Figure 7. Plot of the χ_M vs T for **2** at various fields.

transition with a field up to 50 kOe (inset of Figure 6) including the central loop (step I) around zero and the step at about 4 kOe (step II). A hysteresis loop (inset of Figure 6) is observed clearly when the field is less than 2 kOe, giving a coercive field of 100 Oe and a remnant magnetization of 0.0102 Nβ. And the other loop (step II) can also be observed (Figure S3, Supporting Information).

The low-temperature magnetic phenomena ($T < 10$ K) for **2** were further scrutinized by applying various magnetic fields, as depicted in Figure 7. The peaks in χ_M vs T plots are observed in fields below 4000 Oe and disappear above 6000 Oe. The χ_M value decreases with the increase of the magnetic fields above 5.6 K, which is associated with the spin canting behavior. Below 5.6 K, the 200 Oe curve lays out in an AF interaction. The first spin-canting (step I) takes place in the range of 400−2000 Oe, and the second spin-canting (step II) occurs around 4000 Oe.

From the above study, it can be concluded that compound **2** is a spin-canted weak ferromagnet. As we know, the spin-canting behavior is due to the single-ion magnetic anisotropy or antisymmetric interactions.[46,44] The magnetic behavior of compound **2** may originate from the single-ion anisotropy of Mn(III) and possible structural phase transition at low temperatures, since the occurrence of an antisymmetric or D−M interaction is forbidden because of the presence of an inversion center between Mn ions with space group $P\bar{1}$.[42a,44c,45]

Conclusion

In conclusion, three 1D Mn(III) coordination polymers have been synthesized and characterized structurally and magnetically. Due to the stability of the auxiliary ligands, a series of different chain structures with similar structures was obtained. They are all bridged by the end-to-end mode and connected by weak interacions, which lead to the formation of supramolecular 2D sheet structures. By the introduction of the chiral atoms and substituents, the complexes display different magnetic properties. In complexes **1** and **3**, overall AF exchange interactions are observed, and no long-range ordering exists above 2.0 K. Compound **2** behaves as a rare two-step spin-canted weak ferromagnet with $T_N = 5.6$ K. This work demonstrates that the introduction of substituents could result in varied lower dimensional structures, which is expected to provide more novel model compounds to investigate fascinating magnetic behaviors.

Acknowledgment. We are grateful for financial support from the Natural Science Foundation Council of China (NSFC; grant no. 20401003), 111 Project (B07012), NSFC (90922033), and the National Basic Research Program of China (2009CB929403).

Supporting Information Available: Temperature dependence plot, ZFC−FC plot, and hysteresis as well as a crystallographic information file. This material is available free of charge via the Internet at http://pubs.acs.org.

(45) (a) Jia, H.-P.; Li, W.; Ju, Z.-F.; Zhang, J. *Chem. Commun.* **2008**, *3*, 371. (b) Authier, A. *International Tables for Crystallography*; Kluwer Academic Publishers: Dordrecht, The Netherlands, 2003; Vol. D: Physical Properties of Crystals, pp 127−132. (c) Pfeiffer, S.; Jansen, M. *Z. Anorg. Allg. Chem.* **2007**, *633*, 2558. (d) Wyrzykowski, D.; Warnke, Z.; Kruszyński, R.; Kak, J.; Mroziński, J. *Trans. Metal Chem.* **2006**, *31*, 765.